

**Polarized inelastic neutron scattering of the partially ordered Tb<sub>2</sub>Sn<sub>2</sub>O<sub>7</sub>**K. C. Rule,<sup>1</sup> G. Ehlers,<sup>2</sup> J. R. Stewart,<sup>3</sup> A. L. Cornelius,<sup>4</sup> P. P. Deen,<sup>3</sup> Y. Qiu,<sup>5,6</sup> C. R. Wiebe,<sup>7,8</sup> J. A. Janik,<sup>7</sup> H. D. Zhou,<sup>7</sup> D. Antonio,<sup>4</sup> B. W. Woytko,<sup>4</sup> J. P. Ruff,<sup>9</sup> H. A. Dabkowska,<sup>9</sup> B. D. Gaulin,<sup>9</sup> and J. S. Gardner<sup>5,10,\*</sup><sup>1</sup>*Hahn-Meiner Institut, Glienicker Strasse 100, 14109 Berlin, Germany*<sup>2</sup>*Spallation Neutron Source, Oak Ridge National Laboratory, Oak Ridge, Tennessee 37831-6475, USA*<sup>3</sup>*Institut Laue-Langevin, 6 rue Jules Horowitz, Boîte Postale 156, 38042 Grenoble Cedex 9, France*<sup>4</sup>*University of Nevada, Las Vegas, Nevada 89154-4002, USA*<sup>5</sup>*NCNR, National Institute of Standards and Technology, Gaithersburg, Maryland 20899-8562, USA*<sup>6</sup>*University of Maryland, College Park, Maryland 20742, USA*<sup>7</sup>*Department of Physics, Florida State University, Tallahassee, Florida 32306-3016, USA*<sup>8</sup>*National High Magnetic Field Laboratory, Florida State University, Tallahassee, Florida 32306-4005, USA*<sup>9</sup>*Department of Physics and Astronomy, McMaster University, Hamilton, Ontario L8S 4M1, Canada*<sup>10</sup>*Indiana University, 2401 Milo B. Sampson Lane, Bloomington, Indiana 47408, USA*

(Received 17 August 2007; published 21 December 2007)

We present inelastic neutron scattering results on the geometrically frustrated pyrochlore Tb<sub>2</sub>Sn<sub>2</sub>O<sub>7</sub>. At high temperature  $T > 50$  K, this system resembles the cooperative paramagnet Tb<sub>2</sub>Ti<sub>2</sub>O<sub>7</sub>, while at low temperature  $T \sim 60$  mK, it displays remarkably different behavior. Powder neutron scattering, susceptibility, and specific heat techniques have shown that below 0.87 K Tb<sub>2</sub>Sn<sub>2</sub>O<sub>7</sub> enters a partially ordered state that is characterized by two-sublattice ferrimagnetic long-range order which coexists with paramagnetic spin components. We show that (i) the low-temperature state produces a large internal field and collective excitations and (ii) the coexisting paramagnetic state persists down to 0.1 K, with spins fluctuating at a rate greater than 0.04 THz, resulting in a diffuse magnetic background to the diffraction patterns. A low-lying excitation at 1.2 meV partially softens as short-range correlations build up while cooling in the paramagnetic state.

DOI: [10.1103/PhysRevB.76.212405](https://doi.org/10.1103/PhysRevB.76.212405)

PACS number(s): 75.25.+z, 75.40.Cx, 75.40.Gb, 75.50.Ee

The competition between interactions of similar energy scales is a central theme of many areas of science including biophysics and condensed matter physics.<sup>1</sup> In modern magnetism this has manifested itself in the study of spin glasses and other frustrated magnets. Over the past 10 years a considerable body of work has been performed on geometrically frustrated magnets, although these were first investigated in the 1950s.<sup>2,3</sup>

Rare-earth (RE) titanate pyrochlores RE<sub>2</sub>Ti<sub>2</sub>O<sub>7</sub> have recently attracted the majority of this attention due to the large spin of the RE ion, different spin anisotropies, small exchange constants, and the availability of large single crystals.<sup>4,5</sup> Depending on the RE ion (all other elements are nonmagnetic) the stable ground states range from conventional long-range order<sup>6</sup> and partially ordered states<sup>7</sup> to cooperative paramagnetism.<sup>8</sup> Theoretically, antiferromagnetically (AFM) coupled spins on the pyrochlore lattice should remain dynamic down to the lowest temperatures<sup>9</sup> and with local  $\langle 111 \rangle$  Ising anisotropy the system should enter a non-collinear antiferromagnetic state,<sup>10</sup> as in the case of FeF<sub>3</sub>.<sup>11</sup> However, many enter a spin-glass-like state and the only true cooperative paramagnet is Tb<sub>2</sub>Ti<sub>2</sub>O<sub>7</sub>,<sup>8,9</sup> even with its local anisotropy. Ferromagnetically (FM) coupled spins in this configuration also enter a disordered state with the well-defined, local spin ice structure.<sup>12</sup> Although the bulk properties of all the titanates are well established, slow spin dynamics, ubiquitous to many frustrated magnets, is still poorly understood.<sup>7,8,13–15</sup>

To gain a more detailed understanding of the magnetic ground state, recent studies have perturbed the system via the application of extreme pressures,<sup>16</sup> high magnetic fields,<sup>17</sup>

dilution of the magnetic sublattice,<sup>18</sup> and “stuffing” the RE ions into the lattice.<sup>19</sup>

Studies of isostructural compounds have also been performed, including those of RE stannates,<sup>20–23</sup> where again only the RE ion is magnetic. While the RE sublattice is comparable, Ti<sup>4+</sup>/Sn<sup>4+</sup> substitution can dramatically change the magnetic properties of the system. For example, Gd<sub>2</sub>Sn<sub>2</sub>O<sub>7</sub> has only one transition and a classical long-range-ordered ground state while Gd<sub>2</sub>Ti<sub>2</sub>O<sub>7</sub> has two transitions<sup>7,22</sup> leading to partial order. No freezing has been observed in Er<sub>2</sub>Sn<sub>2</sub>O<sub>7</sub>, while Er<sub>2</sub>Ti<sub>2</sub>O<sub>7</sub> orders via an order-by-disorder transition.<sup>13</sup> On the other hand, the spin ices appear to be very stable with Ti/Sn substitution.<sup>23–25</sup> Both isostructural Tb compounds exhibit AFM correlations at high temperatures, but differences appear at low temperatures. While Tb<sub>2</sub>Ti<sub>2</sub>O<sub>7</sub> remains a cooperative paramagnet down to the lowest temperatures, competing AFM and FM correlations drive Tb<sub>2</sub>Sn<sub>2</sub>O<sub>7</sub> below 0.87 K into a long-range-ordered state.

In the work by Mirebeau and co-workers,<sup>26</sup> low-temperature neutron diffraction and specific heat studies revealed a static, albeit finite-sized, “ordered spin ice state”—i.e., large clusters of a canted ferromagnet, with a canting angle of 13.3° to the local  $\langle 111 \rangle$  axes (this model was confirmed by Dalmas de Réotier *et al.*<sup>27</sup>). A difference in the magnitude of the moment deduced from specific heat and neutron diffraction data and the intense diffuse scattering in the diffraction pattern<sup>28</sup> led Mirebeau *et al.*<sup>26,29</sup> to conclude that the ordered state coexists with slow collective fluctuations in the time scale of 10<sup>−4</sup>–10<sup>−8</sup> s down to mK temperatures.

More recently, however, muon studies by Dalmas de Réotier *et al.*<sup>27</sup> and Bert *et al.*<sup>30</sup> make the case for a dynamic,

rather than static, ground state in  $\text{Tb}_2\text{Sn}_2\text{O}_7$ . The key arguments in their papers centered upon the lack of a precession signal in the muon spin relaxation ( $\mu\text{SR}$ ) measurements and the temperature independence of the muon polarization across the phase transition. The authors of Ref. 27 resolve this apparent contradiction by observing that neutron diffraction is a “faster” technique than  $\mu\text{SR}$ : They argue that both neutron and muon data are consistent with a characteristic spin relaxation time of  $\sim 10^{-10}$  s, significantly faster than that reported earlier by Mirebeau *et al.*<sup>26,29</sup> This claim is remarkable because the only dynamics consistent with the spin correlation functions deduced by neutron diffraction are essentially coherent rotations or tunneling of the magnetization vector. Such dynamics are highly unexpected and of great interest, and should therefore be tested rigorously.

In this paper, we reexamine the nature of the spin system in  $\text{Tb}_2\text{Sn}_2\text{O}_7$ . We will show that below 0.87 K a magnetic state is established that one can describe as a two-sublattice ferrimagnetic long-range-ordered state which coexists with paramagnetic spin components. A significant amount of the spin system ( $5.8 \pm 0.1$ )  $\mu_B$  is static but there is also strong, diffuse magnetic scattering with a liquidlike structure factor originating from  $\approx 3\mu_B$  of fluctuating spins moving faster than 0.04 THz.

Polycrystalline samples of  $\text{Tb}_2\text{Sn}_2\text{O}_7$  were prepared by firing, in air at 1375 °C, stoichiometric amounts of  $\text{Tb}_4\text{O}_7$  and  $\text{SnO}_2$ . High-resolution powder neutron and x-ray diffraction confirmed the high quality and phase purity of the sample.  $\text{Tb}_2\text{Sn}_2\text{O}_7$  is an insulator which crystallizes in the cubic-face-centered space group  $Fd\bar{3}m$  with lattice parameter  $a = 10.426(3)$  Å at 300 K. The paramagnetic properties of  $\text{Tb}_2\text{Ti}_2\text{O}_7$  and  $\text{Tb}_2\text{Sn}_2\text{O}_7$  are very similar. The Curie-Weiss law describes the temperature dependence of the magnetic susceptibility of  $\text{Tb}_2\text{Sn}_2\text{O}_7$  (and  $\text{Tb}_2\text{Ti}_2\text{O}_7$ ) down to  $\sim 50$  K, yielding a Curie-Weiss temperature of  $-10.5$  K ( $-19$  K) and an effective paramagnetic moment of  $9.70(1)\mu_B$  ( $9.40\mu_B$ ) close to the  $9.72\mu_B$  expected for the  $^7\text{F}_6$  free ion. These similarities are not too surprising since the  $\text{Tb}^{3+}$  environments are essentially the same. There is only a 3% difference in the lattice parameter.

Polarized neutron scattering measurements were performed at the D7 time-of-flight spectrometer at the Institut Laue-Langevin. Full three-directional ( $XYZ$ ) neutron polarization analysis<sup>31</sup> was used in order to separate the magnetic scattering from nuclear-coherent, nuclear-spin-incoherent, and background contributions. An incident wavelength of 4.8 Å was chosen with a pyrolytic graphite monochromator. Inserting a Fermi chopper into the incident beam of D7 permits one to perform polarization analysis with energy discrimination over a wide range in  $\mathbf{Q}$  and  $\omega$ . Inelastic neutron scattering measurements (unpolarized) were carried out with both high and low energy resolution on the Disk Chopper Spectrometer (DCS) at NIST. With incident neutron wavelengths between 1.8 and 9 Å, an energy resolution between 1.97 and 0.017 meV was achievable.

Figure 1 shows the magnetic scattering from  $\text{Tb}_2\text{Sn}_2\text{O}_7$  at 60 mK. The diffraction pattern reveals magnetic Bragg peaks at 1.03, 1.2, 1.7, and 2.0 Å<sup>-1</sup>, consistent with earlier results.<sup>26,27</sup> Fitting the Bragg intensities to the ordered spin-

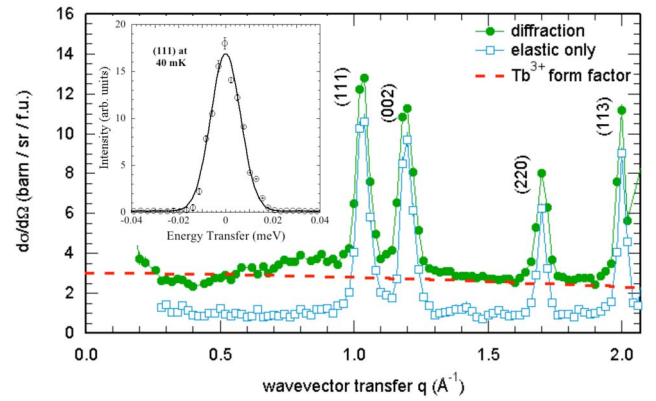


FIG. 1. (Color online) Magnetic neutron diffraction at 60 mK from  $\text{Tb}_2\text{Sn}_2\text{O}_7$ . The solid symbols represent the diffraction pattern (integration over all energy transfers) while the open symbols represent elastic data under the same conditions with an energy window of  $\pm 0.15$  meV. The line is an estimate of the diffuse magnetic scattering; see text. A constant- $\mathbf{Q}$ , high-energy resolution, scan of the magnetic (111) Bragg peak is shown in the inset.

ice model proposed by Mirebeau *et al.*<sup>26</sup> resulted in a static moment of  $(5.8 \pm 0.1)\mu_B$ , again consistent with the previously published data.<sup>26,27</sup> Note that the  $|\mathbf{Q}|$  resolution here does not allow us to see the domain structure reported by others.<sup>26,27</sup> In diffraction one measures the dynamic structure factor  $S(\mathbf{Q}, \omega)$  integrated over all energies from  $-\infty$  to  $E_i$  ( $=3$  meV, in this experiment). With the Fermi chopper in place, elastic scattering ( $-0.15 \text{ meV} < \hbar\omega < 0.15 \text{ meV}$ ) can be measured. This has the full Bragg intensity but the broad diffuse background is significantly suppressed. The broad, liquidlike structure factor in the diffraction pattern is therefore due to spins fluctuating at rates greater than  $\sim 0.04$  THz ( $1 \text{ meV} \approx 0.242 \text{ THz}$ ). Without more data at lower  $|\mathbf{Q}|$  one can only estimate the amount of magnetic moment that gives rise to this broad diffuse scattering. By fitting the high- $|\mathbf{Q}|$ , diffuse magnetic intensity, with the  $\text{Tb}^{3+}$  form factor squared and extrapolating it to  $S(|\mathbf{Q}|=0)$ , one gets  $3\mu_B$ . Combining the two experimentally determined components to the electronic  $\text{Tb}^{3+}$  spins results in a total moment of  $6.5\mu_B$ . This is significantly lower than the free  $\text{Tb}^{3+}$  moment ( $9.72\mu_B$ ); however, we do not expect the full moment because D7 does not integrate over a large enough  $\mathbf{Q}$  or  $\omega$  window, and crystal field effects will reduce the moment.<sup>32</sup>

High-energy resolution data from the DCS are shown in the inset. The magnetic (111) Bragg reflection is resolution limited [full width at half maximum (FWHM) of  $17.0(3) \mu\text{eV}$ ] and should be considered *static*. However, if one were to insist on a dynamical component to this peak, an upper limit of  $\sim 100$  MHz can be put on any fluctuations contributing to the intensity of the peak. This implies that any spin fluctuations must be *slower* than  $10^{-8}$  s; otherwise, a significant amount of broadening would have been observed. This time scale for the spin fluctuations is at the upper limit of Mirebeau *et al.*<sup>26,29</sup>

Three dispersionless magnetic modes at 1.2(1), 10.5(4), and 14.8(4) meV were measured in  $\text{Tb}_2\text{Sn}_2\text{O}_7$  in the paramagnetic phase (not shown). These are reminiscent of the

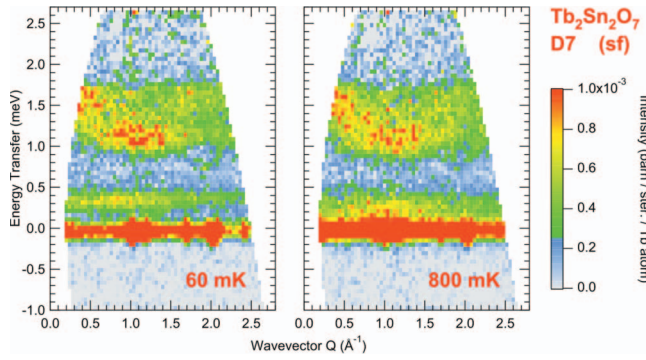


FIG. 2. (Color) Polarized time of flight showing only the spin flip channel from D7. Left panel: 60 mK spectrum revealing a  $\mathbf{Q}$ -independent, low-lying excitation at 0.35 meV (0.085 THz). Right panel: the sample at 800 mK, just below the transition where the quasielastic line is broader (cf. 60 mK data set) but no low-lying mode is seen. At both temperatures the 1.2-meV mode is very soft at the first antiferromagnetic correlation wave vector. In the high-temperature paramagnetic state, this is a  $\mathbf{Q}$ -independent mode.

three lowest excitations seen in  $\text{Tb}_2\text{Ti}_2\text{O}_7$ , where crystalline electric field levels have been measured at 1.2, 10.3, and 14.4 meV.<sup>34</sup> In Fig. 2 the lowest mode can be seen softening at a wave vector of  $\sim 1.1 \text{ \AA}^{-1}$  (the first antiferromagnetic correlation wave vector); this begins as the temperature is lowered below 20 K (not shown), but the system remains gapped as shown down to 60 mK. The similarity in these data and those of  $\text{Tb}_2\text{Ti}_2\text{O}_7$  suggests that the energy scales and crystal field Hamiltonian of both systems are almost identical.

At 800 mK both the quasielastic scattering and 1.2 meV mode are significantly broader than the instrumental resolution. As the system cools further the quasielastic scattering is significantly weaker, magnetic Bragg peaks increase in intensity, and a dispersionless inelastic mode at  $\hbar\omega \sim 0.35 \text{ meV}$  is clearly resolved. All these characteristics are reminiscent of the scattering seen in the field-induced order state of  $\text{Tb}_2\text{Ti}_2\text{O}_7$  reported by some of the authors earlier.<sup>17</sup> Sharp dispersive magnons at  $\approx 1.2 \text{ meV}$  were also seen in the ordered state of  $\text{Tb}_2\text{Ti}_2\text{O}_7$ . Taking constant- $\mathbf{Q}$  cuts through the 60 mK data of  $\text{Tb}_2\text{Sn}_2\text{O}_7$  reveals three modes at 1.07(3), 1.45(3), and 1.60(4) meV (not shown). However, the powder averaging of  $S(|\mathbf{Q}|, \omega)$ , obtained naturally in this experiment, does not allow us to measure a dispersion relationship of these collective excitations.

Recent field-dependent heat capacity measurements were made using a standard thermal relaxation method with the sample attached to an alumina platform. The zero-field data agree well with those already published; that is,  $C_p$  starts to upturn just below 2 K and there is a well-defined peak at  $T_c$ . The  $C/T$  data were fit using a second-order polynomial to model the magnetic plus lattice contribution along with an  $A/T^3$  hyperfine contribution. The  $A$  term can be used to determine the internal field at the nucleus as  $A \propto H_{\text{int}}^2$ . The temperature range of the fits was limited to  $T < 1 \text{ K}$  (except for  $\mu_0 H_{\text{app}} < 1 \text{ T}$  for  $\text{Tb}_2\text{Sn}_2\text{O}_7$  where 0.6 K was used as the upper limit) where the hyperfine contribution was a significant proportion of the total heat capacity. The results are

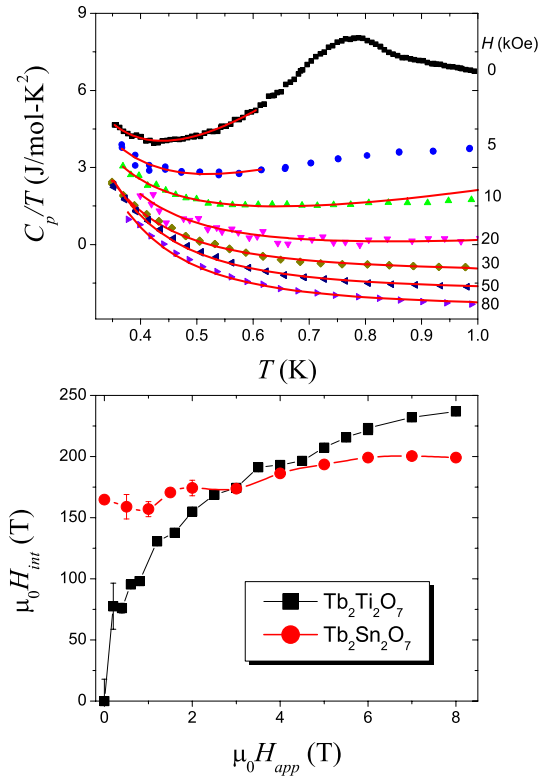


FIG. 3. (Color online) Top panel: low-temperature heat capacity data in several applied magnetic fields. Each data set has been displaced down by  $0.5 \text{ J/(mol K}^2\text{)}$  for clarity. Fits to the nuclear Schottky anomaly at low temperatures (see text) are used to calculate the internal field induced at the  $\text{Tb}^{3+}$  site by its local environment. Lower panel: the calculated internal fields of  $\text{Tb}_2\text{Sn}_2\text{O}_7$  and  $\text{Tb}_2\text{Ti}_2\text{O}_7$  as a function of applied field.

shown in Fig. 3. In the top panel the experimental data and the appropriate fits are shown at several applied fields. The lower panel plots the calculated internal field as a function of applied field. For comparison the same analysis has been carried out on  $\text{Tb}_2\text{Ti}_2\text{O}_7$  and the results are shown in the lower panel. In zero field,  $\text{Tb}_2\text{Ti}_2\text{O}_7$  is still very dynamic and no net field is observed; however, in  $\text{Tb}_2\text{Sn}_2\text{O}_7$  an internal field of  $\approx 160 \text{ T}$  was calculated. This large field (typical for ordered rare-earth magnets) is only reached in  $\text{Tb}_2\text{Ti}_2\text{O}_7$  when  $\approx 2 \text{ T}$  is applied and earlier neutron scattering studies<sup>17</sup> indicate that  $\text{Tb}_2\text{Ti}_2\text{O}_7$  is ordered.

In conclusion, the paramagnetic high-temperature regimes of  $\text{Tb}_2\text{Ti}_2\text{O}_7$  and  $\text{Tb}_2\text{Sn}_2\text{O}_7$  have very similar characteristics. Both systems obey the Curie-Weiss law over a wide temperature range above 50 K. However, as the systems are cooled into the spin-correlated region, differences begin to appear. While  $\text{Tb}_2\text{Ti}_2\text{O}_7$  remains dynamic down to the lowest temperatures, we have conclusively revealed the presence of static and dynamic spins in  $\text{Tb}_2\text{Sn}_2\text{O}_7$  at 60 mK. At least 60% of the total possible spin system is static and contributes to large magnetic Bragg peaks and a nuclear Schottky anomaly. These static spins produce an internal field and collective excitations in a similar manner to applying 2 T to  $\text{Tb}_2\text{Ti}_2\text{O}_7$ . The other part of the spin system is dynamic (faster than  $\sim 0.04 \text{ THz}$ ) and contributes to the liquidlike diffuse scattering of the diffraction patterns.



A two-component spin system is not uncommon in geometrically frustrated magnets, where omnipresent spin dynamics often persists to the lowest temperatures. Normally it is a small part of the spin system which remains dynamic, and in  $\text{Tb}_2\text{Sn}_2\text{O}_7$  we estimate it at around 30%. Mirebeau *et al.*<sup>29</sup> have come up with a plausible argument for an effective ferromagnetic coupling in  $\text{Tb}_2\text{Sn}_2\text{O}_7$  where dipolar interactions overcome the superexchange, but then one would rather expect  $\text{Tb}_2\text{Sn}_2\text{O}_7$  to become a spin ice or a well-ordered compound like  $\text{Ho}_2\text{Ru}_2\text{O}_7$ .<sup>35</sup> We have provided inelastic neutron scattering results on  $\text{Tb}_2\text{Sn}_2\text{O}_7$  revealing a similar energy landscape to that in  $\text{Tb}_2\text{Ti}_2\text{O}_7$ , pointing out the importance of AFM correlations. The results presented in this paper will hopefully stimulate further experimental and theoretical studies in this material, especially the growth of

single crystals so that vital information like nearest-neighbor and next-nearest-neighbor exchange interactions can be measured.

It is a pleasure to acknowledge the support and hospitality of the ILL and NIST facilities during the neutron experiments and the many discussions with S. T. Bramwell, P. M. Bentley, and V. Garcia-Sakai. The state of Florida partially funded this work. Work at the Spallation Neutron Source (SNS) and UNLV are supported under U.S. Department of Energy (DOE) Contracts Nos. DE-AC05-00OR22725 and DE-FC52-01NV14049, respectively. This work utilized facilities supported in part by the National Science Foundation under Agreements Nos. DMR-0454672 and DMR-0084173.

\*Corresponding author. jsg@nist.gov

<sup>1</sup>See, for example, *Frustrated Spin Systems*, edited by H. T. Diep (World Scientific, Singapore, 2004).

<sup>2</sup>G. H. Wannier, Phys. Rev. **79**, 357 (1950).

<sup>3</sup>P. W. Anderson, Phys. Rev. **102**, 1008 (1956).

<sup>4</sup>J. E. Greedan, J. Alloys Compd. **408**, 444 (2006).

<sup>5</sup>J. S. Gardner, B. D. Gaulin, and D. M. Paul, J. Cryst. Growth **191**, 740 (1998).

<sup>6</sup>A. L. Cornelius, B. E. Light, Ravhi S. Kumar, M. Eichenfield, T. Dutton, R. Pepin, and J. S. Gardner, Physica B **359-361**, 1243 (2005).

<sup>7</sup>J. R. Stewart, G. Ehlers, A. S. Wills, S. T. Bramwell, and J. S. Gardner, J. Phys.: Condens. Matter **16**, L321 (2004).

<sup>8</sup>J. S. Gardner, S. R. Dunsiger, B. D. Gaulin, M. J. P. Gingras, J. E. Greedan, R. F. Kiefl, M. D. Lumsden, W. A. MacFarlane, N. P. Raju, J. E. Sonier, I. Swainson, and Z. Tun, Phys. Rev. Lett. **82**, 1012 (1999).

<sup>9</sup>J. Villain, Z. Phys. B **33**, 31 (1979).

<sup>10</sup>B. C. den Hertog and M. J. P. Gingras, Phys. Rev. Lett. **84**, 3430 (2000).

<sup>11</sup>G. Ferey *et al.*, Rev. Chim. Miner. **23**, 474 (1986).

<sup>12</sup>S. T. Bramwell and M. J. P. Gingras, Science **294**, 1495 (2001).

<sup>13</sup>J. Lago, T. Lancaster, S. J. Blundell, S. T. Bramwell, F. L. Platt, M. Shirai, and C. Baines, J. Phys.: Condens. Matter **17**, 979 (2005).

<sup>14</sup>J. A. Hodges, P. Bonville, A. Forget, and G. Andre, Can. J. Phys. **79**, 1373 (2001).

<sup>15</sup>G. Ehlers, A. L. Cornelius, M. Orendac, M. Kajnakova, T. Fennell, S. T. Bramwell, and J. S. Gardner, J. Phys.: Condens. Matter **15**, L9 (2003).

<sup>16</sup>I. Mirebeau, I. N. Goncharenko, P. Cadavez-Pares, S. T. Bramwell, M. J. P. Gingras, and J. S. Gardner, Nature (London) **420**, 54 (2002).

<sup>17</sup>K. C. Rule, J. P. C. Ruff, B. D. Gaulin, S. R. Dunsiger, J. S. Gardner, J. P. Clancy, M. J. Lewis, H. A. Dabkowska, I. Mirebeau, P. Manuel, Y. Qiu, and J. R. D. Copley, Phys. Rev. Lett. **96**, 177201 (2006).

<sup>18</sup>A. Keren, J. S. Gardner, G. Ehlers, A. Fukaya, E. Segal, and Y. J. Uemura, Phys. Rev. Lett. **92**, 107204 (2004).

<sup>19</sup>G. C. Lau, R. S. Freitas, B. G. Ueland, B. D. Muegge, E. L. Duncan, P. Schiffer, and R. J. Cava, Nat. Phys. **2**, 249 (2006).

<sup>20</sup>V. Bondah-Jagalu and S. T. Bramwell, Can. J. Phys. **79**, 1381

(2001).

<sup>21</sup>K. Matsuhira, Y. Hinatsu, K. Tenya, H. Amitsuka, and T. Sakakibara, J. Phys. Soc. Jpn. **71**, 1576 (2002).

<sup>22</sup>P. Bonville, J. A. Hodges, M. Ocio, J. P. Sanchez, P. Vulliet, S. Sosin, and D. Braithwaite, J. Phys.: Condens. Matter **15**, 7777 (2003).

<sup>23</sup>K. Matsuhira, Y. Hinatsu, K. Tenya, and T. Sakakibara, J. Phys.: Condens. Matter **12**, L649 (2000).

<sup>24</sup>Hiroaki Kadowaki, Yoshinobu Ishii, Kazuyuki Matsuhira, and Yukio Hinatsu, Phys. Rev. B **65**, 144421 (2002).

<sup>25</sup>S. T. Bramwell, M. J. Harris, B. C. den Hertog, M. J. P. Gingras, J. S. Gardner, D. F. McMorrow, A. R. Wildes, A. Cornelius, J. D. M. Champion, R. G. Melko, and T. Fennell, Phys. Rev. Lett. **87**, 047205 (2001).

<sup>26</sup>I. Mirebeau, A. Apetrei, J. Rodriguez-Carvajal, P. Bonville, A. Forget, D. Colson, V. Glazkov, J. P. Sanchez, O. Isnard, and E. Suard, Phys. Rev. Lett. **94**, 246402 (2005).

<sup>27</sup>P. Dalmas de Reotier, A. Yaouanc, L. Keller, A. Cervellino, B. Roessli, C. Baines, A. Forget, C. Vaju, P. C. M. Gubbens, A. Amato, and P. J. C. King, Phys. Rev. Lett. **96**, 127202 (2006).

<sup>28</sup>Broad features in magnetic neutron diffraction are often interpreted as scattering from dynamic spins; however, static disordered spins cannot be ruled out.

<sup>29</sup>I. Mirebeau, A. Apetrei, I. N. Goncharenko, and R. Moessner, Physica B **385-386**, 307 (2006).

<sup>30</sup>F. Bert, P. Mendels, A. Olariu, N. Blanchard, G. Collin, A. Amato, C. Baines, and A. D. Hillier, Phys. Rev. Lett. **97**, 117203 (2006).

<sup>31</sup>O. Schärpf and H. Capellmann, Phys. Status Solidi A **135**, 359 (1993).

<sup>32</sup>In  $\text{Tb}_2\text{Ti}_2\text{O}_7$  Gingras *et al.* (Ref. 33) have calculated that  $\text{Tb}^{3+}$  possesses  $\sim 5\mu_B$  due to crystal field effects.

<sup>33</sup>M. J. P. Gingras, B. C. den Hertog, M. Faucher, J. S. Gardner, S. R. Dunsiger, L. J. Chang, B. D. Gaulin, N. P. Raju, and J. E. Greedan, Phys. Rev. B **62**, 6496 (2000).

<sup>34</sup>J. S. Gardner, B. D. Gaulin, A. J. Berlinsky, P. Waldron, S. R. Dunsiger, N. P. Raju, and J. E. Greedan, Phys. Rev. B **64**, 224416 (2001).

<sup>35</sup>C. R. Wiebe, J. S. Gardner, S. J. Kim, G. M. Luke, A. S. Wills, B. D. Gaulin, J. E. Greedan, I. Swainson, Y. Qiu, and C. Y. Jones, Phys. Rev. Lett. **93**, 076403 (2004).